SciEn

Proceedings of 8th International Conference on Mechanical, Industrial and Energy Engineering 2024
02-04 January, 2025, Khulna, BANGLADESH

SciEn Conference Series: Engineering Vol. 3, 2025, pp 643-648 https://doi.org/10.38032/scse.2025.3.161

Effect of Rayleigh number on Heat Transfer Characteristics of Finned Heat sink

Oishi Kanta[*], *Md Abdullah Al Mohotadi, Khandkar Aftab Hossain*

Department of Mechanical Engineering, Khulna University of Engineering & Technology, Khulna-9203, Bangladesh

ABSTRACT

In the present work, the performance of a vertical rectangular fin array based on a horizontal heat sink is analyzed for various Rayleigh number with increasing heating power by numerical analysis of steady state natural convection heat transfer. The continuity, momentum, and energy equations are solved using three-dimensional numerical simulations with FLUENT software to forecast the flow and temperature field with air as working medium. Governing equations are discretized and evaluated throughout the solid heat sink and fluid air computational domain. Fins made of aluminum with a high thermal conductivity were chosen for better heat dissipation. The enhancement of temperature differentials between the fluid domain and heat sink causes the Rayleigh number to rise with increased heating power. Using fixed fin base length, the declining character of thermal resistance, enhancement of heat transfer coefficients and Nusselt numbers were analyzed for Rayleigh numbers ranging from 4×10^6 to 20×10^6. The temperature increases across the heat sink array, reaches to maximum in the middle, and then progressively releases the heat through the fins bodies into the surrounding air. Fluid flow and thermal structure between the transverse and longitudinal fin channels as well as along the entire fin array were depicted. Two different kinds of flow patterns were identified in the fin arrays channel, and the temperature flow had a parabolic structure.

Keywords: Natural Convection, Heat Sink, Rayleigh Number, Buoyancy Force, Thermal Resistance.

1. Introduction

In many scientific and technological domains, thermal energy is the most significant aspect. The operation of many engineering systems results in the generation of heat. The heat generated by the operation of many electronic and mechanical devices will prevent the efficient and safe operation of these devices. For this reason, the heat generated within a system must be dissipated to its surrounding in order to maintain the system operating at its recommended working temperatures and functioning effectively and reliably [1]. Natural convection heat transfer is crucial in air heat exchangers utilized across several sectors [2, 3].

A multitude of scholars have investigated natural convection heat transfer through both computational and experimental methods and continue to engage in this field of study [4, 5, 6, 7]. A heat sink functions passively in electrical systems by effectively absorbing or dissipating thermal energy from the surroundings via extended surfaces such as fins and spines. Heat sinks are utilized in numerous applications requiring effective heat dissipation [8]. Sertkaya et al. [9] determined that inline pin fin and plate heat sinks perform most effectively when oriented upwards, with an optimal number of pins. The experimental dataset was analyzed regarding parametric effects, leading to the composition and proposal of empirical correlation expressions. Jones and Smith [10] examined how fin height and fin spacing influence the heat transfer coefficient. The conclusion drawn indicates that fin spacing serves as the primary geometrical parameter, and it is recommended to select it as the characteristic length. Baskaya et al. [11] demonstrated that short fins outperform long fins. Overall, the value of the heat transfer coefficient decreases with fin length as a result of changes in the flow patterns. Ghandouri et al. [12, 13] found that corrugated fins and rippling fins demonstrate superior cooling performance when compared to rectangular fins, resulting in a lower base temperature than heatsinks utilizing rectangular fins. Yu et al. [14] compared the impact of fin number, length, height, and heat flux on thermal resistance and heat transfer coefficient using parametric experiments. Increased fin number, length, and height result in lower thermal resistance and heat transfer coefficient. The authors suggested a correlation to forecast the average Nusselt number for radial heat sinks. Initially, Elenbaas [15] advocated modifying the Ra number for a rectangular plate fin. The adjustment was based on the assumption that flow between stretched surfaces resembles internal duct flow. Nemati et al. [16] introduced a new expression for Ra to account for the presence of a finned tube. This revised phrasing aligns better with flow patterns. We presented a new correlation for Nusselt number using the modified Rayleigh number and compared it to prior correlations.

In this work, a rectangular finned heat sink is numerically simulated using a three dimensional finite volume approach for a variety of Rayleigh numbers by varying heating powers. The simulation aims to describe fluid dynamics through and around the heat sink fins, which are not apparent in the investigation of earlier literature. Compared to earlier research, a more thorough explanation of the heat transfer coefficient, Nusselt number, and temperature contours for both transverse and longitudinal directions is presented. Also the flow configurations that take place in the fin array channels are analyzed in this study.

*Corresponding Author Email Address: oishikanta@gmail.com

2. Numerical Modeling

2.1 Heat sink geometry

The physical model is constructed using ANSYS Spaceclaim. **Fig.1** shows the geometry and **Table 1** represents the corresponding dimension used in the model.

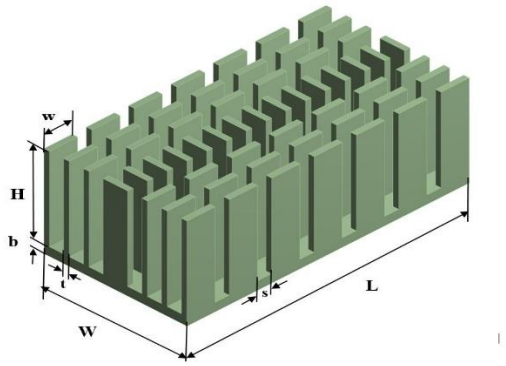

Fig. 1 Heat Sink Geometry

TABLE 1 Dimensions used for the simulation model

Parameters		Heat Sink
Fin Base Length (mm)		150
Fin Base Width (mm)		76
Fin Base Height (mm)		5
Fin Width (mm)		9
Fin Height (mm)		35
Fin Thickness (mm)		3
Fin Spacing (mm)	Transverse	8.17
	Longitudinal middle fins	7.5
	Longitudinal side fins	14.5
Number of Fins		57

Seven different Rayleigh numbers will be applied at the base of heat sink with convection in walls and a simulation zone will be created around the heat sink for evaluating heat transfer in computational model. In order to reduce the amount of computational resources, the following assumptions will be made:

i. The air flow is steady, three-dimensional and no-slip on the fin surface.

ii. Boussinesq model is used in air zone.

iii. Except density, the properties of air are constant and properties are constant for fin material.

iv. Radiation heat loss is negligible.

2.2 Main equations

Continuity equation:

$$\frac{\partial(\rho u)}{\partial x}+\frac{\partial(\rho v)}{\partial y}+\frac{\partial(\rho w)}{\partial z}=0 \quad (1)$$

Momentum equation:

$$\rho\left(u\frac{\partial u}{\partial x}+v\frac{\partial u}{\partial y}+w\frac{\partial u}{\partial z}\right)=-\frac{\partial P}{\partial x}+\mu\nabla^2 u \quad (2)$$

$$\rho\left(u\frac{\partial v}{\partial x}+v\frac{\partial v}{\partial y}+w\frac{\partial v}{\partial z}\right)=-\frac{\partial P}{\partial y}+\mu\nabla^2 v+(\rho-\rho_0)g \quad (3)$$

$$\rho\left(u\frac{\partial w}{\partial x}+v\frac{\partial w}{\partial y}+w\frac{\partial w}{\partial z}\right)=-\frac{\partial P}{\partial z}+\mu\nabla^2 w \quad (4)$$

Energy equation:

$$\frac{\partial(\rho uT)}{\partial x}+\frac{\partial(\rho vT)}{\partial y}+\frac{\partial(\rho wT)}{\partial z}=\frac{k}{c_p}\left(\frac{\partial^2 T}{\partial x^2}+\frac{\partial^2 T}{\partial y^2}+\frac{\partial^2 T}{\partial z^2}\right) \quad (5)$$

Model for solid region:

There is no internal heat source in the heat sink, so the energy equation of the solid region can be written as:

$$\frac{\partial^2 T}{\partial x^2}+\frac{\partial^2 T}{\partial y^2}+\frac{\partial^2 T}{\partial z^2}=0 \quad (6)$$

For natural-convection flow, the simulation can get quick convergence with the Boussinesq model,

$$\rho=\rho_0[1-\beta(T-T_0)] \quad (7)$$

Where, ρ is air density at temperature T, ρ_0 is air density at T_0, β is air thermal expansion coefficient.

2.3 Grid generation

A 3D steady-state numerical domain is developed and analyzed using ANSYS Fluent. A triangular coarse mesh having an element size of 1.3 mm for the heatsink and 8.6 mm for the fluid region is utilized in the meshing process to facilitate modifications to the meshing approach. The heatsink is integrated inside the fluid region. The mesh density next to the fin surface is augmented if $Y^+ < 1$. **Fig. 2** shows the generated mesh in the heat sink.

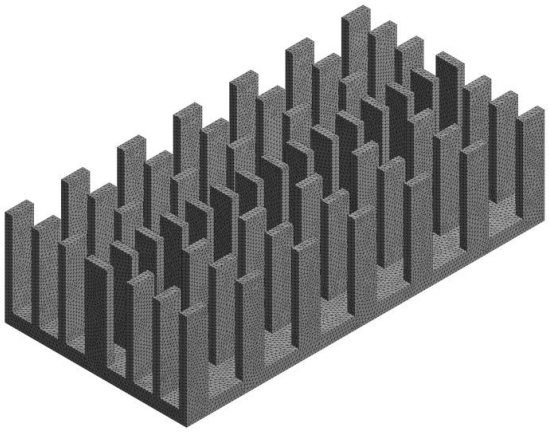

Fig. 2 Generated mesh in 3D model

3. Result and Discussion

3.1 Grid independency test and model validation

The numerical study is conducted using several meshing algorithms, and the average temperatures at the surface of the fin are observed and compared. The outcomes of the simulation are presented in **Fig. 3**, indicating that the optimal meshing approach corresponds to a grid number of 5,266,863.

The results of heat transfer coefficients obtained validates the conventional plate fin heat sink is demonstrated in **Fig. 4** [17]. The observed findings exhibit a consistent trend, confirming their validity, with minor variations attributed to grid size, operating conditions, and geometrical factors. In conclusion, these comparisons indicate that the existing model is applicable for predicting flow and heat distributions for the present issue.

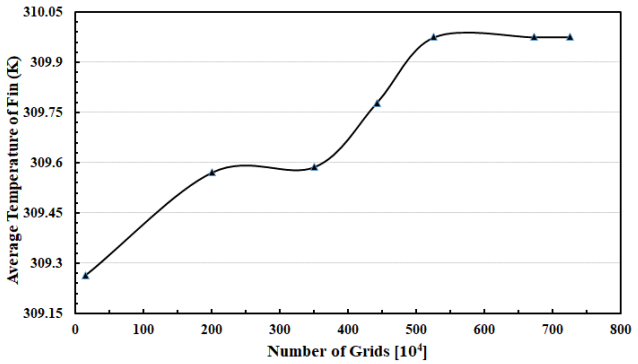

Fig. 3 Grid Independency Test

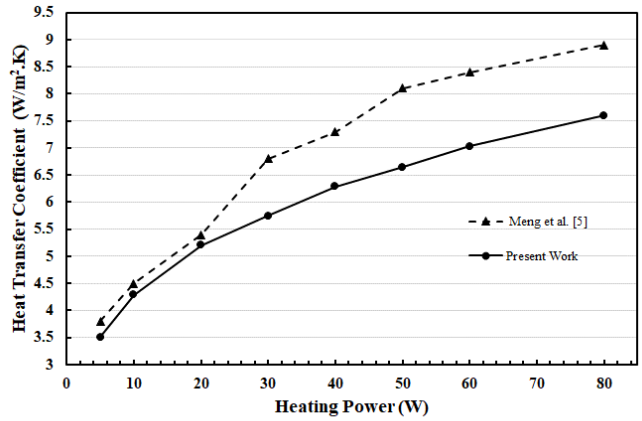

Fig. 4 Numerical Model Validation

3.2 Temperature distribution of fin arrays along transverse and longitudinal direction

Fig. 5 represents the temperature contours for the aluminum heat sink for heating power 10, 30 and 60 Watts at different coordinates (XY and YZ planes). It can be observed that, increase in heating power causes an increase in temperature throughout the body of the heat sink. The maximum temperature region can be noticed at the central part of the heat sink which dissipates into the surroundings gradually though the fin arrays. From the temperature contours of transverse and longitudinal direction, heat dissipation into the surroundings in a parabolic shape are seen. As the temperature drops at a higher rate from the side walls of the fins than the middle, this phenomenon is created. With increasing heating power, natural convection augments, since temperature difference between the heat sink and air domain enhances [18].

3.3 Temperature distribution along fin channel

In order to visualize the heat flow in the channel of the fin arrays, temperature distributions at different cross-sections in the fin channel are plotted for 10, 30 and 60 Watts. In **Fig. 6**, It is clear that the temperature at the fin walls is higher than the inter fin region. The air in contact with the hot walls of the fin arrays is heated which causes the air density to decrease, eventually flowing the air along the vertical fins. From the temperature contours along transverse and longitudinal fin channels, it can be observed that air in the transverse fin channel takes up more heat from two sides of the heated surfaces of fin walls than air in the longitudinal fin channel. Due to this reason more buoyancy force is generated within air of the transverse fin channel [19]. Also as the heat input increases, it promotes the rise in fin region temperature (both transverse and longitudinal) because temperature increases all over the body of the heat sink.

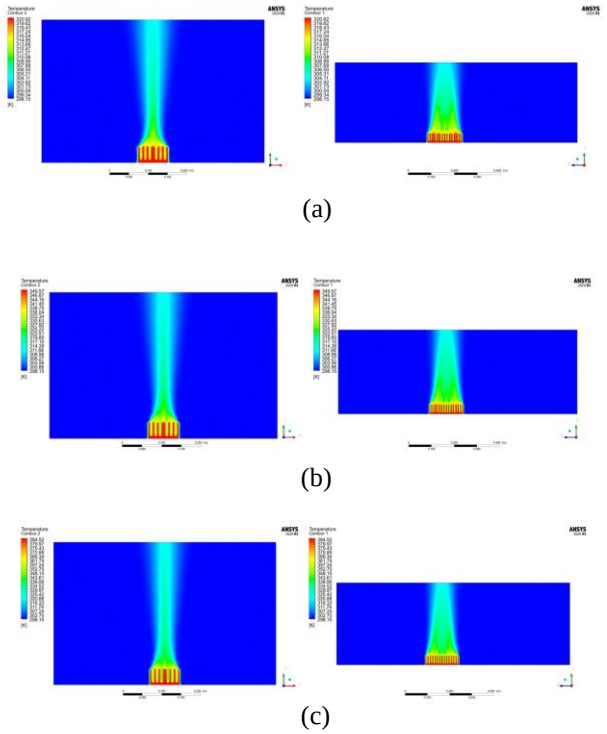

(a)

(b)

(c)

Fig. 5 Temperature contours along transverse and longitudinal directions
(a) For 10W, (b) For 30W, (c) For 60W

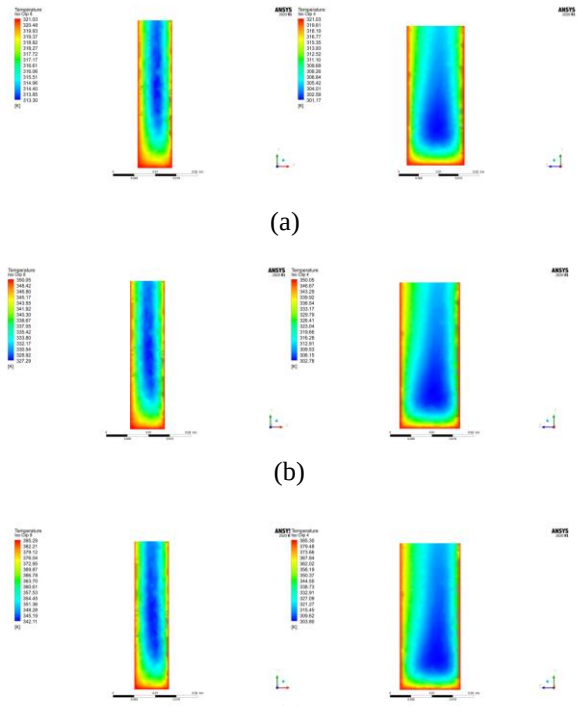

(a)

(b)

(c)

Fig. 6 Temperature contours along Fin Channels (transverse and longitudinal)
(a) For 10W, (b) For 30W, (c) For 60W

3.4 Velocity distribution along transverse and longitudinal direction of fin arrays

In **Fig. 7** velocity vectors are shown for 10, 30 and 60 Watts in transverse and longitudinal directions. As heating power increases, air temperature increases causing a reduction in air density which enhances the buoyant force. This indicates that the velocity in the top region was greater than in the lower region of the heat sink, demonstrating that the warmer air ascended. For this enhancement, air velocity increases with heating power. Also, air velocity is seen to be high near the central part of the heat sink since maximum temperature is generated at the mid region and middle side of the heat sink has a lower heat dissipation rate than the side wall [18].

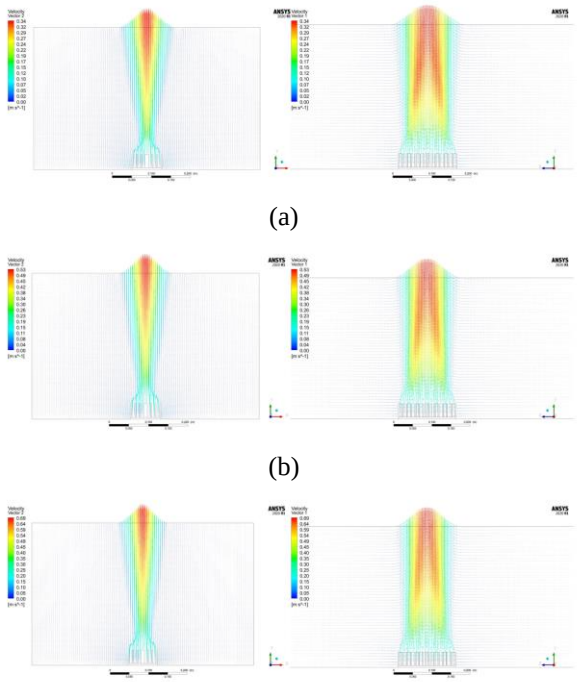

(a)

(b)

(c)

Fig. 7 Velocity vectors along transverse and longitudinal directions
(a) For 10W, (b) For 30W, (c) For 60W

3.5 Velocity distribution along fin channel

To examine the flow within the fin array channels, airflow patterns at various cross-sections are illustrated in **Fig. 8**. From the contours, it can be seen that air velocity is zero at the proximity of the fin walls. Two distinct sorts of flow patterns have appeared in the channels of the fin array. In the transverse fin channel, air flows from the open ends, traverses the length, and exits at the channel's center. Compared to the velocity components along fin length and height, the velocity component along fin spacing is substantially smaller which causes a single chimney type flow pattern within transverse fin channel [20]. As heating input increases, air velocity also augments and it shifts from single chimney type to up and down flow pattern in the transverse fin channel.

With a wide fin spacing, cold air can enter the longitudinal channel of the fin array from the middle section between the fins, turn almost 180 degrees and travel up the fin height to the channel center. Thus an up and down flow pattern is created here which can be seen in **Fig. 9**. Since all velocity components combine to generate the flow in the longitudinal fin channel, this kind of flow is completely three-dimensional. Air velocity increases as heating input increases, and a more up-and-down flow pattern is seen [20]. Comparing air velocities between longitudinal and transverse directions, it can be concluded that air velocity is more in transverse than longitudinal fin channel because air in the longitudinal fin channel absorbs less heat from the two sides of the heated fin wall surfaces.

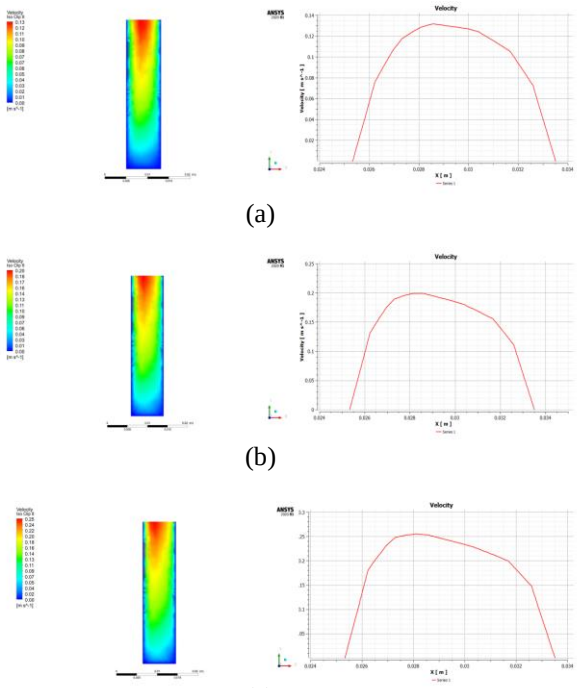

(a)

(b)

(c)

Fig. 8 Velocity contours and magnitudes along transverse fin channel
(a) For 10W, (b) For 30W, (c) For 60W

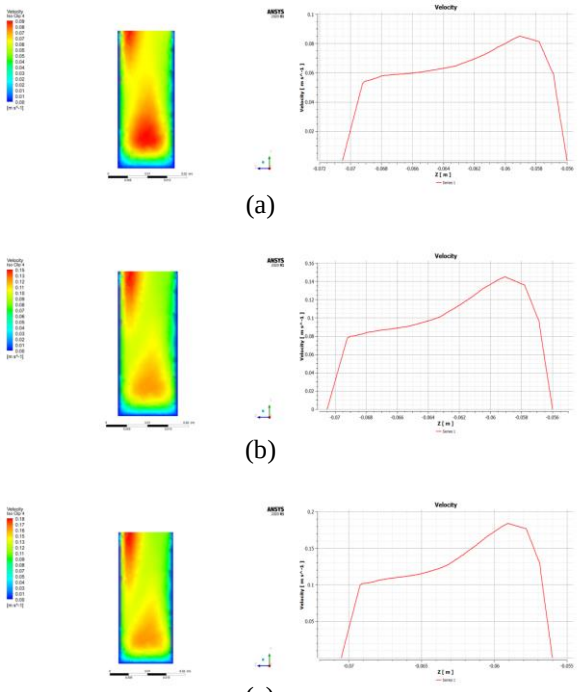

(a)

(b)

(c)

Fig. 9 Velocity contours and magnitudes along longitudinal fin
(a) For 10W, (b) For 30W, (c) For 60W

3.6 Analysis of heat transfer characteristics

In order to assess the behavior of heat transfer, this study evaluated thermal resistance for a variety of input factor combinations. Effective heat sinks minimize thermal

resistance by maximizing heat transfer to the environment. **Fig. 10** illustrates the relationship between heating power and thermal resistance. When heating power increases, thermal resistance decreases [17]. The heat transfer coefficient fluctuation with heating input is seen in the **Fig. 11**. It is evident that a higher heat input results in a higher average heat transfer coefficient. It happens because the temperature differential between the air domain and the heat sink widens with increasing heat input, which promotes free convective heat transfer. The reason for this is as heat flows from the heated layer to the air's outer layers.

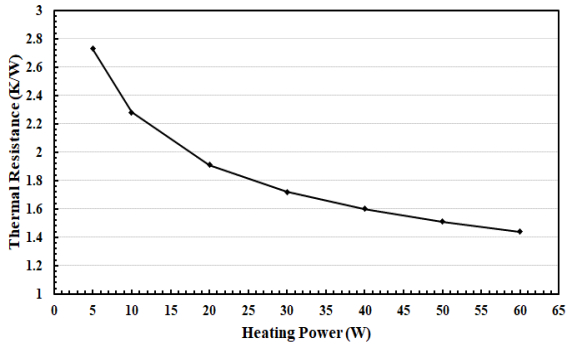

Fig. 10 Thermal Resistance variation with Heating Power

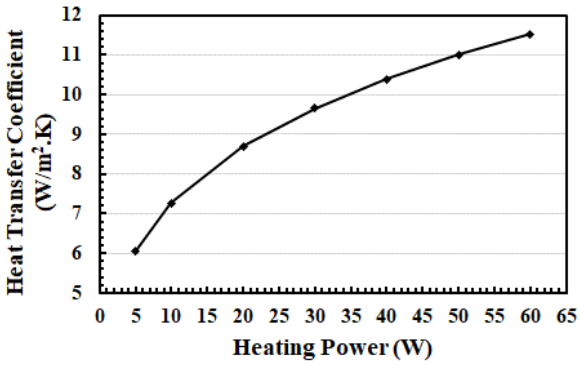

Fig. 11 Heat Transfer Coefficient at different Heating Power

Fig. 12 depicts how the Nusselt number for natural convection is influenced by the Rayleigh number. Nu is clearly improved by raising the Ra. Since temperature gradients grow with increasing heat input, the Rayleigh number and heat transfer coefficients are enhanced [18].

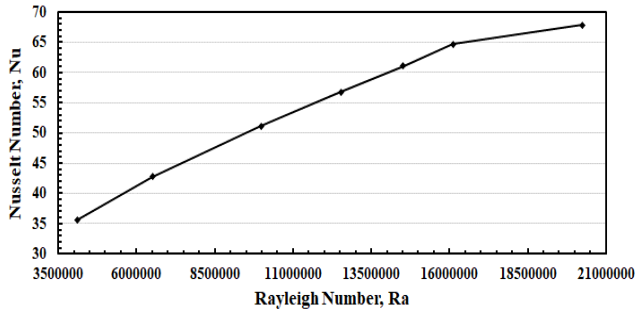

Fig. 12 Nusselt Number Variation with Rayleigh Number

4. Conclusion

The heat transfer characteristics of horizontal rectangular fin arrays were studied with natural convection. The temperature contours, velocity contours, and in-channel fluid flow patterns were analyzed throughout this present work. The results showed that when Rayleigh number increased, the average heat transfer coefficient and Nusselt number also increased. Natural convection is increased by raising the heat flux because it causes a greater temperature differential between the air domain and the heat sink fin array. Temperature contours show the parabolic temperature profile because of higher heat dissipation from side wall of the fin array than mid region. Buoyancy force is found to be dominant in transverse fin channel. Single chimney type fluid flow pattern is noticed along the longitudinal fin channel and up and down flow pattern is observed along transverse fin channel. With increasing heating power, air temperature augments which causes air density to decrease and boosts the buoyant force, the main mechanism for dissipating the increasing heat by natural convection cooling. As the heating power increases leading to variation in Rayleigh number, the thermal resistances show a declining nature.

5. Acknowledgement

The authors express gratitude for the support from the Department of Mechanical Engineering, Khulna University of Engineering and Technology (KUET), Khulna.

References

[1] Hitit University, Dept. of Mechanical Engineering, Çorum, Türkiye, M. Kaya, Ş. Kaya, and Keçiören Industrial Vocational School, Ankara, Türkiye, "Optimum fin spacing of rectangular fins on aluminum heat sinks plates," *Proc. Romanian Acad. Ser. Math. Phys. Tech. Sci. Inf. Sci.*, vol. 24, no. 2, pp. 151–157, Nov. 2023.

[2] L. Micheli, K. S. Reddy, and T. K. Mallick, "Thermal effectiveness and mass usage of horizontal micro-fins under natural convection," *Appl. Therm. Eng.*, vol. 97, pp. 39–47, Mar. 2016.

[3] I. Tari and M. Mehrtash, "Natural convection heat transfer from horizontal and slightly inclined plate-fin heat sinks," *Appl. Therm. Eng.*, vol. 61, no. 2, pp. 728–736, Nov. 2013.

[4] E. Hahne and D. Zhu, "Natural convection heat transfer on finned tubes in air," *Int. J. Heat Mass Transf.*, vol. 37, pp. 59–63, Mar. 1994.

[5] C.-S. Wang, M. M. Yovanovich, and J. R. Culham, "Modeling Natural Convection From Horizontal Isothermal Annular Heat Sinks," *J. Electron. Packag.*, vol. 121, no. 1, pp. 44–49, Mar. 1999.

[6] V. I. Terekhov, A. L. Ekaid, and K. F. Yassin, "Laminar free convection heat transfer between vertical isothermal plates," *J. Eng. Thermophys.*, vol. 25, no. 4, pp. 509–519, Oct. 2016.

[7] M. Yaghoubi and M. Mahdavi, "An Investigation of Natural Convection Heat Transfer from a Horizontal Cooled Finned Tube," *Exp. Heat Transf.*, vol. 26, no. 4, pp. 343–359, Aug. 2013.

[8] H. Lee, *Thermal Design: Heat Sinks, Thermoelectrics, Heat Pipes, Compact Heat Exchangers, and Solar Cells*. John Wiley & Sons, 2022.

[9] A. A. Sertkaya, M. Ozdemir, and E. Canli, "Effects of pin fin height, spacing and orientation to natural convection heat transfer for inline pin fin and plate heat sinks by experimental investigation," *Int. J. Heat Mass Transf.*, vol. 177, p. 121527, Oct. 2021.

[10] C. D. Jones and L. F. Smith, "Optimum Arrangement of Rectangular Fins on Horizontal Surfaces for Free-Convection Heat Transfer," *J. Heat Transf.*, vol. 92, no. 1, pp. 6–10, Feb. 1970.

[11] S. Baskaya, M. Sivrioglu, and M. Ozek, "Parametric study of natural convection heat transfer from horizontal rectangular fin arrays," *Int. J. Therm. Sci.*, vol. 39, no. 8, pp. 797–805, Sep. 2000.

[12] I. E. Ghandouri, A. E. Maakoul, S. Saadeddine, and M. Meziane, "Thermal performance of a corrugated heat dissipation fin design: A natural convection numerical analysis," *Int. J. Heat Mass Transf.*, vol. 180, p. 121763, Dec. 2021.

[13] I. El Ghandouri, A. El Maakoul, S. Saadeddine, and M. Meziane, "Design and numerical investigations of natural convection heat transfer of a new rippling fin shape," *Appl. Therm. Eng.*, vol. 178, p. 115670, Sep. 2020.

[14] S.-H. Yu, K.-S. Lee, and S.-J. Yook, "Natural convection around a radial heat sink," *Int. J. Heat Mass Transf.*, vol. 53, no. 13, pp. 2935–2938, Jun. 2010.

[15] W. Elenbaas, "Heat dissipation of parallel plates by free convection," *Physica*, vol. 9, no. 1, pp. 1–28, Jan. 1942.

[16] H. Nemati, M. Moradaghay, S. A. Shekoohi, M. A. Moghimi, and J. P. Meyer, "Natural convection heat transfer from horizontal annular finned tubes based on modified Rayleigh Number," *Int. Commun. Heat Mass Transf.*, vol. 110, p. 104370, Jan. 2020.

[17] X. Meng, J. Zhu, X. Wei, and Y. Yan, "Natural convection heat transfer of a straight-fin heat sink," *Int. J. Heat Mass Transf.*, vol. 123, pp. 561–568, Aug. 2018.

[18] H. S. Sultan, K. B. Saleem, B. M. Alshammari, M. Turki, A. Aydi, and L. Kolsi, "Numerical investigation of natural convection from a horizontal heat sink with an array of rectangular fins," *Case Stud. Therm. Eng.*, vol. 61, p. 104877, Sep. 2024.

[19] I. El Ghandouri, A. El Maakoul, S. Saadeddine, and M. Meziane, "Design and numerical investigations of natural convection heat transfer of a new rippling fin shape," *Appl. Therm. Eng.*, vol. 178, p. 115670, Sep. 2020.

[20] M. Mobedi and H. Yüncü, "A three dimensional numerical study on natural convection heat transfer from short horizontal rectangular fin array," *Heat Mass Transf.*, vol. 39, no. 4, pp. 267–275, Apr. 2003.

NOMENCLATURE

Nu : Nusselt Number
Ga : Grashof Number
Pr : Prandlt Number
Ra : Rayleigh Number
h : Heat Transfer Coefficient, W/m^{2}K
R_{th} : Thermal Resistance, K/W
Q_{hs} : Heat Dissipation Power, W
ρ : Variable Air Density, kg/m^3
ρ_0 : Air Density at 25°C, kg/m^3